A novel formulation of multi-component drop evaporation models for spray applications

S. Tonini, G.E. Cossali

September 29, 2014

Abstract

An analytical model predicting the evaporation rate for multi-component liquid drops is proposed, taking into account the effect of all mass diffusivities within the gas phase. The increment of the evaporation rate due to gas convection is included according to the film theory. The model is validated against experimental measurements for bi and tri-component motionless drops. A simpler model, based on the single-component analogy, is also proposed and compared to other simplified models from the open literature, with good agreement.

1 Nomenclature

B_M	Spalding mass transfer number	-
D	*species* diffusion coefficient	m^2/s
$\dot{m}_{ev}$	evaporation rate	kg/s
M_m	molar mass	$kg/kmol$
P	pressure	Pa
P_v	vapour pressure	Pa
r	radial distance	m
$\bar{R}$	*universal* gas constant	$J/kmolK$
Re	Reynolds number	-
R_V	equivalent drop radius	m
R_0	drop radius	m
Sc	Schmidt number	-
Sh	Sherwood number	-
T	temperature	K
U	velocity	m/s

Greek symbols

α		-
χ	mass fraction	-
φ	volume fraction	-
ρ	density	kg/m^3
σ	Lennarde-Jones length	m
Ω_D	collision integral	-
ε	evaporation rate fraction	-

Subscripts

c convective

ref reference

s drop surface

∞ ambient conditions

Superscripts

j, k index

m mixture

T total

v vapour

2 Introduction

The evaporation of liquid droplets into a gaseous environment is a process extensively employed in many engineering processes and it has been of great interest to engineers since decades [1]. In many applications (internal combustion engine, aeronautical sectors, to cite a few) the evaporating liquid droplets contain many components with different thermodynamic properties. As petroleum fuels, such as gasoline and diesel, but also biofuels, are *blends of as many as 300 components [2]*, an approach that takes into account the inter-diffusivity among all the evaporating species to model the complex fuel vaporization process is opportune.

The influence of different volatilities of the numerous components in practical multi-component liquids still needs to be understood [3], since it may play significant roles in the rate of heating and vaporization of spray droplets.

The trend in future internal combustion engines is to be operated under low-temperature combustion conditions for NO_x emissions reduction [4]; under these conditions, the earlier vaporisation of *high volatility* components is enhanced affecting the ignition and combustion processes, while heavier components vaporizing later will affect the emission formation [5]. Consequently, multicomponent vaporization models are required for more accurate engine simulations.

In the last few decades, extensive research has been carried out on the modelling of multi-component liquid droplet evaporation in a gaseous environment, addressing all the different aspects related to this complex process,

which can be classified into three main topics: thermal and mass transports in the liquid, thermodynamic conditions at the liquid/gas interface, mass diffusion and convection of volatile species within the gas phase.

Only numerical models, based on the *numerical* solution of the Navier-Stokes equations, may deal with all the aforementioned issues, although the computational time required for a simulation makes such approach not suitable for spray investigation. A huge variety of simplified models have then become popular within the scientific community.

Related to the first topic, the models of multi-component droplet heating and evaporation could be subdivided into two main groups: those based on the analysis of individual components, "discrete component models" (refer to [6], [7], [8], [9], [10] for example), which *assume* that a multicomponent fuel is composed of a finite number of components with different properties and *they are* applicable in the case when a small number of components needs to be taken into account, and those based on the probabilistic analysis of a large number of components (e.g. "continuous thermodynamics approach" [11], [12], [13] and the "distillation curve model" [14]). In the second family of models a number of additional simplifying assumptions were used, including the hypothesis that species inside droplets mix infinitely quickly. As a result, the number of variables can be greatly reduced compared to the discrete component approach.

Law and Law [15] proposed a simplified model for multi-component drop evaporation, which represents an analog of the classical spherically symmetric single-component "d^2-law". The model is based on the observation that the extremely slow rate of liquid phase mass diffusion causes the droplet concentration distributions to attain almost constant values during much of the droplet lifetime.

In realistic moving droplets, species diffusion takes place alongside species convection when Hill-type vortices are formed inside droplets [10]. In most practically relevant cases, however, the details of non-symmetric species concentration within the droplet are not important and the effects of mass diffusion and convection can be described in terms of the spherically symmetric effective diffusivity model [1].

As far as the treatment of the liquid-gas interphase, under pressure conditions close to atmospheric, an ideal solution can be assumed for the liquid phase and the gas phase can be approximated as a mixture of ideal gases, then vapour-liquid equilibrium is usually expressed in the form of the Raoult's law [12]. *However, under high pressure conditions, the droplet vaporisation exhibits characteristics that are distinctly different from those in low pressure environments [16], and the treatment of the liquid-phase transport processes should take into account high pressure*

effects (liquid phase solubility of ambient gases, high pressure treatment of liquid phase equilibrium based on the fugacity of each phase, pressure effect on thermo-transport properties). These works are implicitly based on the assumption that both liquid and gas phases can be treated as a continuum, although this hypothesis is no more valid with sub-micrometer droplets. Under these conditions kinetic effects should be considered in the vicinity of the droplet surface; one of the recent development on the modelling of droplet evaporation accounting for such effect is based on the direct numerical solution to the Boltzmann equations for vapours and air in the vicinity of the droplet [17].

The majority of the models available in the literature and developed for spray simulations do not address in details the complex problem of the mass diffusion of multi-component vapour in air [18]. Some of them are based on the assumption that the inter-diffusivity among all the volatile species within the gas phase is orders of magnitude lower compared to the mass diffusivity of each species in air, as suggested in [19]. Moreover the problem can be further simplified assuming that the multi-component vapour can be treated as mono-component, introducing an average diffusion coefficient as in [15], [16], [20]. Recently Zang et al. [5] proposed a numerical solution for the set of equations of a multi-component drop evaporation model, which accounts for the diffusivities of all the species in the gas phase.

The present work has a double target. From one side it proposes an analytical solution to evaluate the evaporation rate of a multi-component liquid drop taking into account the effect of species mass diffusion in the gas phase, then it proposes a novel simplified model, based on the single-component analogy, by introducing a new way to evaluate an average diffusion coefficient for all the species. This second model results to be in closer agreement with the detailed one, making it suitable for spray simulations.

The effect of gas convection on the evaporation rate is taken into account, according to the well accepted evaporation model of Abramzon and Sirignano, which was developed for pure liquids [21] and it is extended here to the multi-component case. This model includes the effect of the Stefan flow on the heat and mass transfer, and it describes the evaporation process even at high transfer rates by making use of the film theory for calculating the Nusselt and Sherwood numbers [22].

The following sections report the mathematical model, the derivation of analytical expressions for the instantaneous evaporation rate from liquid drops, the comparison with the predictions of simpler models available in the open

literature and against data base of experimental measurements. The main conclusions are then briefly summarised.

3 The mathematical model

The present model calculates the evaporation rate for a spherical multi-component liquid drop in quiescent air, assuming steady-state and constant drop radius, uniform gas density and mass diffusion according to the Fick's law. The above mentioned assumptions are common in the majority of drop evaporation models for spray simulations. Some of those assumptions have been recently relieved, for example [23] includes the effect of drop surface receding during evaporation, [24] considers the influence of gas density dependence on temperature and vapour concentration.

The species conservation equations for a spherical droplet in spherical coordinates (and spherical symmetry) are [25]:

$$\frac{d}{dr}\left(r^2\rho U\chi^{(k)} - r^2 D^{(k,m)}\rho\frac{d\chi^{(k)}}{dr}\right) = 0; \quad \text{for } k = 0,..,n \tag{1}$$

where $k = 1,..,n$ represent the n evaporating components, while $k = 0$ represents the inert gas, and $D^{(k,m)}$ is the mass diffusion coefficient for the species k in the gaseous mixture according to the Blanc's law [26]:

$$D^{(k,m)} = \left(\sum_{j=0;\ j\neq k}^{n}\frac{\chi_{ref}^{(j)}}{D^{(k,j)}}\right)^{-1} \tag{2}$$

$D^{(k,j)}$ are the binary diffusion coefficients of species k in species j, $\chi_{ref}^{(j)}$ is the mass fraction of the species j in the gas phase, calculated at reference conditions, according to [27]:

$$\chi_{ref}^{(j)} = \frac{2\chi_s^{(j)} + \chi_\infty^{(j)}}{3} \tag{3}$$

To notice that the flux of the inert gas at $r = R_d$ is nil and consequently the gas mass flux is nil everywhere. The mass fraction of the gas is simply calculated from the unity constrain:

$$\chi^{(0)} = 1 - \sum_{k=1}^{n}\chi^{(k)} \tag{4}$$

From the mass conservation equation:

$$U = \frac{\sum_{k=1}^{n}\dot{m}_{ev}^{(k)}}{4\pi r^2\rho} \tag{5}$$

introducing the non-dimensional coordinate $\zeta = \frac{R_0}{r}$, the solution of the conservation equation for each species (1) assumes the following expression:

$$\chi^{(k)} = \alpha^{(k)}e^{-\frac{\dot{m}_{ev}^{(T)}}{4\pi\rho R_0 D^{(k,m)}}\zeta} + \varepsilon^{(k)} \tag{6}$$

where $\varepsilon^{(k)}$ is the evaporation rate fraction of species k:

$$\varepsilon^{(k)} = \frac{\dot{m}_{ev}^{(k)}}{\sum_{j=1}^{n} \dot{m}_{ev}^{(j)}} \tag{7}$$

and $\alpha^{(k=1,..,n)}$ are constant.

The problem is closed imposing the B.C. at the drop surface and at free stream conditions:

$$\begin{aligned} P_v^{(k)}\left(r = R_0\right) &= P_v^{(k)}\left(\zeta = 1\right) = P_{v,s}^{(k)} \\ \chi^{(k)}\left(r = \infty\right) &= \chi^{(k)}\left(\zeta = 0\right) = \chi_{\infty}^{(k)} \end{aligned} \tag{8}$$

leading:

$$\varepsilon^{(k)} = \frac{\chi_s^{(k)} - \chi_{\infty}^{(k)} e^{-\frac{\dot{m}_{ev}^{(T)}}{4\pi\rho R_0 D^{(k,m)}}}}{1 - e^{-\frac{\dot{m}_{ev}^{(T)}}{4\pi\rho R_0 D^{(k,m)}}}} \tag{9}$$

then, from the condition $\sum_{k=1}^{n} \varepsilon^{(k)} = 1$, the drop total evaporation rate $\dot{m}_{ev}^{(T)}$ can be implicitly calculated solving the non-linear equation:

$$\sum_{k=1}^{n} \frac{\chi_{\infty}^{(k)} - \chi_s^{(k)}}{\left(e^{-\frac{\dot{m}_{ev}^{(T)}}{4\pi\rho R_0 D^{(k,m)}}} - 1\right)} = 1 - \sum_{k=1}^{n} \chi_{\infty}^{(k)} \tag{10}$$

Once the total evaporation rate is obtained, the evaporation rate fraction for each species can be calculated as a cascade routine from the system (9).

The proposed model correctly takes into account the inter-species interaction within the gas phase, calculating the mass diffusion of each species in all the others. The solution of the non-linear equation (10) for $\dot{m}_{ev}^{(T)}$ requires a numerical algorithm with a rather simple implementation, then the set (9) becomes linear and it can be easily solved. This represents a novelty of the present work, compared to previous similar studies, like [5], where instead a numerical solutions of a different non linear system for the calculation of $\dot{m}_{ev}^{(T)}$ and $\varepsilon^{(k)}$ is proposed.

3.1 Evaporation rate under convective conditions

In case of liquid drop evaporating in a convective flow (Re $\neq$ 0), the approach presented here follows the well known model of Abramzon and Sirignano [21], which was developed according to the film theory [22]. The model assumes that the evaporating drop is surrounded by different mass diffusional regions, which thicknesses depend on the physical properties of each species*, based on the hypothesis that the interaction of the evaporating species is small,*

as properly commented in [20]. Moreover the introduction of the Sherwood number for each species $Sh^{(k)}$ allows to relate the evaporation rate for each species under convective conditions to that under non-convective conditions ($\mathrm{Re} = 0$), as described by the following formula:

$$\dot{m}_{ev,c}^{(k)} = \frac{Sh^{(k)}}{2} \dot{m}_{ev}^{(k)} \tag{11}$$

Following [21], $Sh^{(k)}$ can be defined by semi-empirical correlations:

$$\begin{aligned} Sh^{(k)} &= 2 + \frac{Sh_0^{(k)} - 2}{F_M\left(B_M^{(m)}\right)} \\ Sh_0^{(k)} &= 2 + 0.552\sqrt{\mathrm{Re}}\sqrt[3]{Sc^{(k)}} \\ F_M\left(B_M^{(m)}\right) &= \frac{\left(1 + B_M^{(m)}\right)^{0.7} \log\left(1 + B_M^{(m)}\right)}{B_M^{(m)}} \end{aligned} \tag{12}$$

being $Sc^{(k)}$ the Schmidt number for the species k:

$$Sc^{(k)} = \frac{\nu}{D^{(k,m)}} \tag{13}$$

and the mass transfer number for the gaseous mixture is defined as follows:

$$B_M^{(m)} = \frac{\sum_{k=1}^{n} \chi_s^{(k)} - \sum_{k}^{n} \chi_\infty^{(k)}}{1 - \sum_{k=1}^{n} \chi_s^{(k)}} \tag{14}$$

From the previous relations, the following results can be obtained. First the drop total evaporation rate under convective conditions $\left(\dot{m}_{ev,c}^{(T)}\right)$ can be simply correlated to the total evaporation rate $\left(\dot{m}_{ev}^{(T)}\right)$ and evaporation rate fractions $\left(\varepsilon^{(k)}\right)$ under non convective conditions:

$$\dot{m}_{ev,c}^{(T)} = \frac{\sum_{k=1}^{n} Sh^{(k)} \varepsilon^{(k)}}{2} \dot{m}_{ev}^{(T)} \tag{15}$$

then the evaporation rate fraction for each species under convective conditions $\left(\varepsilon_c^{(k)}\right)$ results a function of the species Sherwood numbers and the evaporation rate fractions under non-convective conditions:

$$\varepsilon_c^{(k)} = \frac{Sh^{(k)} \varepsilon^{(k)}}{\sum_{j=1}^{n} Sh^{(j)} \varepsilon^{(j)}} \tag{16}$$

The following section presents and comments the results obtained with the present model, which accurately takes into account the mass diffusion of each species in the gaseous mixture, and the comparison with previous mathematical expressions available in the scientific literature. Moreover a new simplified model predicting the evaporation rate for multi-component liquid drops is proposed and compared.

4 Results and discussions

The section presents the results from the parametrical analysis, under steady-state conditions, of the proposed multi-component drop evaporation model, which takes into account the interaction of mass diffusion of each species in the gas phase. Simplified correlations, which neglect the effect of inter-species mass diffusion, are proposed and their results are compared to the ones obtained with the more detailed model proposed here.

Finally the model predictions, under transient conditions, are compared with the results from the experimental data base of [28], for bi- and tri-component drops evaporating in stagnant environment.

4.1 Steady-state drop evaporation

A parametrical analysis is performed to enlighten the effect of different operating conditions on the drop evaporation rate as predicted by the present model, which mathematical derivation has been described in the previous section, and by other simplified models available in the open literature.

These models suggested a more simple solution for the problem of mass transport into the gas phase, either assuming the multi-component mixture as mono-component or neglecting the interaction of each species with the others.

The first simplified model selected for comparison proposes a mathematical expression for the total evaporation rate for multi-component drop in analogy with the mono-component case, as well described in [20]:

$$\dot{m}_{ev}^{(T)\ [Model\ 1]} = 4\pi R_0 \rho_{ref} \bar{D}^{(v,0)} \ln\left(1 + B_M^{(m)}\right) \tag{17}$$

where the mass transfer number for the whole gaseous mixture has the same mathematical expression as equation (14), and $\bar{D}^{(v,0)}$ is the diffusion coefficient of the mean vapour mixture in air, calculated according to the Wilke and Lee formula [29], which takes into account the physical properties of each species :

$$\bar{D}^{(v,0)} = \frac{3.03 - \frac{0.98}{\sqrt{\bar{M}^{(v,0)}}} 10^{-2} T^{3/2}}{P\sqrt{\bar{M}^{(v,0)}} \left(\bar{\sigma}^{(v,0)}\right)^2 \Omega_D} \tag{18}$$

$$\bar{M}^{(v,0)} = \frac{n+1}{\sum_{j=0}^{n} \frac{1}{M_m^{(j)}}} \tag{19}$$

$$\bar{\sigma}^{(v,0)} = \frac{\sum_{j=0}^{n} \sigma^{(j)}}{n+1} \tag{20}$$

where $\sigma^{(j)}$ are the characteristic Lennard-Jones lengths for all the species in the gas phase, and Ω_D is the collision integral, function of temperature, the characteristic Lennard-Jones energies for all the species and the Boltzmann constant (refer to [20] for a complete description of the mathematical formulation)

The model calculates the evaporation rate fraction for each species according to this expression:

$$\varepsilon^{(k)\ [Model\ 1]} = \frac{\chi_s^{(k)}}{\sum_{j=1}^{n} \chi_s^{(j)}} \tag{21}$$

which results to be valid only in case of vapour free conditions at far distance form the drop, $\chi_\infty^{(k=1,n)} = 0$.

The second simplified model selected for the purposes of the present investigation is described in [19], based on the concept that in the gas phase the mass diffusion of each vaporising species in the inert air is orders of magnitude higher than within the other species, then an expression for the evaporation rate for each species is proposed as follows:

$$\dot{m}_{ev}^{(k)\ [Model\ 2]} = 4\pi R_V^{(k)} \rho_{ref} D^{(k,0)} \ln\left(1 + B_M^{(k)}\right) \tag{22}$$

where $R_V^{(k)}$ is the equivalent drop radius, function of the species volume fraction in the liquid mixture $\varphi^{(k)}$:

$$R_V^{(k)} = R_0 \sqrt[3]{\varphi^{(k)}} \tag{23}$$

$D^{(k,0)}$ is the gas diffusivity of pure species k in air at reference condition and $B_M^{(k)}$ is the species mass transfer coefficient, defined as follows:

$$B_M^{(k)} = \frac{\chi_s^{(k)} - \chi_\infty^{(k)}}{1 - \chi_s^{(k)}} \tag{24}$$

Then the drop total evaporation rate and the evaporation rate fraction for each species are simply calculated as:

$$\dot{m}_{ev}^{(T)\ [Model\ 2]} = \sum_{k=1}^{n} \dot{m}_{ev}^{(k)\ [Model\ 2]} \tag{25a}$$

$$\varepsilon^{(k)\ [Model\ 2]} = \frac{\dot{m}_{ev}^{(k)\ [Model\ 2]}}{\dot{m}_{ev}^{(T)\ [Model\ 2]}} \tag{25b}$$

To maintain the advantage of those simple models, a new expression for the total evaporation rate is here proposed, based on the mono-component analogy as suggested by [20], and introducing a different expression for the average mass diffusion coefficient:

$$\dot{m}_{ev}^{(T)\ [Model\ 3]} = 4\pi R_0 \rho_{ref} \bar{D}^{(v,m)} \ln\left(1 + B_M^{(m)}\right) \tag{26}$$

where $B_M^{(m)}$ is calculated according to equation (14), and the average mass diffusion coefficient $\bar{D}^{(v,m)}$ is function of the mass fraction at reference conditions:

$$\bar{D}^{(v,m)} = \frac{\sum_{k=1}^{n} \chi_{ref}^{(k)} D^{(k,m)}}{\sum_{k=1}^{n} \chi_{ref}^{(k)}} \tag{27}$$

The evaporation rate fraction for each species k is calculated according to equation (9), which results to be valid even in case of not vapour free environment, a condition typical in evaporating spray applications.

A parametrical analysis has been performed to compare the results from the detailed model, equation (10), and the three simpler expressions for the total evaporation rate, equations (17), (25a) and (26).

Different multi-component drops have been investigated, which have been collected in four macro-groups. The drop compositions have been chosen from test cases available in the scientific literature [20], [19] and [28].

Table 1 reports the liquid mass fraction of three alcohol and *acetone* bi-component drops, made by three different compositions of ethanol and acetone.

Similarly, table 2 reports the liquid mass fraction of three bi-component drops, made by n-decane and 3-pentanone.

The third group of drop composition is presented in table 3, which reports the liquid volume fraction of drops made by alcohols, alkanes and/or water.

Finally table 4 reports the liquid volume fraction of bi- and tri-component drops made by five different alkanes. This last group of drop compositions has been selected since a detailed experimental data-base is available for model comparison [28].

The results from the parametrical analysis are presented in terms of the ratio between the evaporation rate as predicted by the three simpler expressions (17), (25a) and (26) and the value calculated solving the equation (10):

$$\delta m_{ev}^{[j]} = \frac{\dot{m}_{ev}^{[Model\ j]}}{\dot{m}_{ev}^{[Model\ 0]}} \tag{28}$$

where $\dot{m}_{ev}^{[Model\ 0]}$ is the drop evaporation rate as predicted by the present detailed model, solving equation (10).

The four images of figure 1 show the difference in the evaporation rate among the three simpler expressions and the present model for the different drop compositions reported in the four groups of table 1, 2, 3 and 4. All the test cases correspond to liquid drops at temperature equal to 300 K evaporating in stagnant vapour free environment at 500 K. The results evidence that the newly proposed expression for the evaporation rate, equation (26) of Model 3, is in almost coincident agreement with the detailed model for all the test cases investigated. The first simpler

expression described by equation (17) of Model 1 is in rather good agreement with the present detailed model for the ethanol-acetone group, while the second simpler expression proposed in equation (25a) of Model 2, noticeably underestimates the evaporation rate for all the multi-component drop test cases. To be noticed that the composition D1 and D5 correspond to mono-component drops.

The effect of drop temperature on the evaporation rate is shown in the four images of figure 2, which report only one composition for each of the four groups described in table 1, 2, 3 and 4. The liquid temperature has been varied between 280 K and the boiling temperature of the most volatile species within each of the selected composition, while the gaseous environment, at non-convective vapour free conditions, is fixed equal to 500 K.

The results confirm the very good agreement between the newly proposed simpler expression for the evaporation rate, equation (26) of Model 3, and the more detailed model (10). The first expression, *equation (17) of* Model 1, increasingly deviates from the detailed model as liquid temperature increases, except for the test case from the third group, corresponding to a drop made by 20% methanol, 20% ethanol, 20% 1-butanol, 20% n-heptane and 20% n-decane (test case C2 of table 3), where the differences reduce at higher liquid temperatures. Again the second simpler expression, equation (25a) of Model 2, underestimates the evaporation rate for all the four drop compositions, with the differences increasing with drop temperature, except for the second group with a drop made by 85% n-decane and 15% 3-pentanone.

The effect of gas temperature is presented in figure 3 for all the test case compositions proposed in figure 2.

The drop temperature is fixed equal to 300 K, while the gas temperature has been varied between 300 K and 1000 K.

The results confirm the previous conclusions and they also suggest that there is no effect of gas temperature on the difference between the second and third simpler expressions (Model 2 and Model 3) and the detailed model.

Finally the effect of vapour composition at free stream conditions is presented in figure 4 for two drop compositions from the first and fourth groups (test case A1 and D7, respectively).

The drop and gas temperatures have been fixed equal to 300 K and 500 K, respectively, and the gas is under non-convective conditions.

The vapour mass fraction at free stream conditions of the first species in the drop composition has been varied from 0 up to the corresponding value at drop surface. The results show that this effect becomes noticeably only for

the test case D7 of table 4. This suggests that the detailed model should be preferred in case of fuel spray simulations, where the presence of vaporised fuel in the gas phase, due to the evaporation of different liquid drops, makes the assumption of vapour free environment no more valid.

The proposed parametrical analysis suggests that among the three simplified evaporation models selected, Model 3, with a newly proposed expression for the mean mass diffusion coefficient, is in better agreement with the more detailed model, which correctly takes into account the mass diffusion of each species within the gas phase, for all the selected operating conditions.

4.2 Transient drop evaporation

The following results present the comparison among the present model predictions and the experimental measurements reported in [28] in terms of drop size temporal evolution.

This data-base has been selected among the ones available in the open scientific literature, since it contains all the information necessary to predict the different test-cases. *Single, optically levitated droplets were studied, being this setup suitable for the investigation of evaporation processes which last a long time and where the evaporation rate is low. The droplet was levitated by the radiation force of a continuous light source, using a Nd:YAD laser with a wavelength of 532 nm. In order to avoid heat input from the laser, the droplet liquid must not absorb the light and this requirements is fulfilled in case of n-alkanes. Optical techniques were employed to measure the drop size and temperature. The ambient temperature was measured with thermocouples which uncertainty varies form 0.5 K at 300 K up to 1 K at 350 K. The droplet diameter was measured with a relative uncertainty that depends on the absolute value of the droplet diameter and it was lower than 1.5% for all the measurements.*

The assumption of uniform temperature in the liquid phase is made in all the simulations, justified by the fact that the liquid drop is under levitating low evaporation conditions. Consequently the infinite conductivity model is implemented in the present analysis. Refer to [1] for a comprehensive review on the modelling of drop thermal diffusion, where the assumption of uniform temperature within the liquid phase is relaxed.

The calculations have been stopped when the drop diameter has been reduced down to 1/10 of the initial size.

Only the predictions using the present accurate model are reported since, under the selected operating conditions which correspond to low drop evaporation rate, the simpler Model 1 and Model 3 (equations (17) and (26), respectively)

predict almost coinicident values of Model 0, while the simpler Model 2 (equation (25a)) clearly underestimates the evaporation rate.

Figure 5 shows the transient profile of non-dimensional drop surface as function of the reduced time (defined as $t/\left(2R_0\right)^2$) for different compositions of thetradecane/hexadecane levitating drops, vaporising in stagnant vapour free air at 304 K. The initial composition of liquid drops correspond to the test cases D1÷D5 of table 4. The results enlighten the rather good agreement among the model predictions (lines) and the experimental measurements (symbols). Furthermore the figure shows that the profiles corresponding to the two limiting mono-component compositions are according to the "d^2-law", while the bi-component test cases present a non-linear profile. When the more volatile species is almost totally evaporated the slope of the profile corresponds to the test case with the heavier mono-component species.

This conclusion is enlightened in figure 6(a), which shows the transient evolution of the drop size together with the drop composition for the test case with the initial liquid mass fraction of thetradecane equal to 0.8 (test case D2 of table 4). The change of slope in the non-dimensional drop size profile corresponds to the time when the more volatile species is practically completed evaporated. Figure 6(b) reports the transient profiles of the instantaneous evaporation rate for the two vaporising species, showing the monotonic decreasing in the case of the lighter component, while the evaporation rate of the heavier component, which initially is almost two orders of magnitude lower, reaches a maximum at the time when the liquid concentration of the other one has almost totally disappeared.

The evaporation behaviour for two levitating three-component drops vaporizing in stagnant air is presented in figure 7. The initial composition of the liquid drops corresponds to the test cases D6 and D7 of table 4, while air temperature at free stream conditions is fixed equal to 299.8 K and 296.2 K, respectively. To be notice that the two graphs of figure 7 are reported in semi-logarithm scale.

Again the comparison among model predictions (line) and experimental measurements (symbols), as shown in figure 7(a), is in good agreement for the two test cases, except at larger times for the drop with heavier components (test case D7), where however also the experimental data are missing.

Figure 7(b) presents the time evolution of drop size and composition for the test case D7, confirming that the changes of slope in the drop size profile correspond to the time when the mass fraction of the more volatile components practically disappears.

These results confirm that the proposed analytical model of multi-component drop evaporation, which accounts for the inter-species mass diffusion in the gaseous mixture, predicts the evaporation rate for a wide range of operating conditions showing a rather good agreement with the selected experimental data base.

5 Conclusions

An analytical model of multi-component drop evaporation is proposed, accounting for the inter-species mass diffusion in the gaseous mixture. The proposed model accurately calculates the fraction of each species evaporation rate even in case of not vapour free environment.

A simpler model, based on the single-component analogy, is also suggested where a new definition of the mean mass diffusion coefficient is used; the results are in excellent agreement with the more accurate solution. However in case of spray simulations, particularly with alkanes, the more accurate model, which correctly takes into account the inter-species mass diffusion, should be preferred.

The model is used to predict the transient evolution of drop size for bi- and tri-component levitating drops evaporating in stagnant air under low evaporation rate conditions and the results are in rather good agreement with the available experimental data.

6 Figures

Figure 1: Comparison between simplified multi-component drop evaporation models and the present detailed one for all the test cases of table 1, 2, 3 and 4.

Figure 2: Effect of drop temperature on the comparison between simplified multi-component drop evaporation models and the present detailed one; test cases A1, B1, C2 and D7, $T_\infty = 500\ K$, Re $= 0$, $\chi_\infty^{(k=1,n)} = 0$.

Figure 3: Effect of gas temperature on the comparison between simplified multi-component drop evaporation models and the present detailed one; test cases A1, B1, C2 and D7, $T_s = 300\ K$, Re $= 0$, $\chi_\infty^{(k=1,n)} = 0$.

Figure 4: Effect of vapour mass fraction at free stream conditions on the comparison between simplified multi-component drop evaporation models and the present detailed one; test cases A1 and D7, $T_s = 300\ K$, $T_\infty = 500\ K$, Re $= 0$.

Figure 5: Comparison between model predictions (lines) and experimental measurements of [28] (symbols) of non-dimensional drop size temporal evolution for five n-thetradecane/n-hexadecane drops with different initial composition; test cases D1÷D5, $R_0 = 25\ \mu m$, $T_\infty = 304\ K$, Re = 0.

Figure 6: Temporal evolution of (a) non-dimensional drop size and species volume fraction concentration and (b) instantaneous evaporation rates for an n-thetradecane/n-hexadecane drop; test cases D2, $R_0 = 25\ \mu m$, $T_\infty = 304\ K$, Re = 0, $\varphi_{l,0}^{(n-C_{14}H_{30})} = 0.8$.

Figure 7: (a) Comparison between model predictions (lines) and experimental measurements of [28] (symbols) of non-dimensional drop size temporal evolution for two alkane drops with different initial composition; test cases D6 and D7, Re = 0, $R_0 = 25\ \mu m$, $T_\infty = 299.8\ K$ (case D6) and $T_\infty = 296.2\ K$ (case D7). (b) temporal evolution of non-dimensional drop size and species volume fraction concentration for test cases D7, $R_0 = 25\ \mu m$, $T_\infty = 299.9\ K$, Re = 0.

7 Tables

Table 1: Initial mass fraction composition of alcohol and ketone or two-component drops.

Table 2: Initial mass fraction composition of hydrocarbon and ketone for two-component drops.

Table 3: Initial volume fraction composition of alcohol, hydrocarbon and water for four- and five-component drops.

Table 4: Initial volume fraction composition of hydrocarbons or two- and three-component drops.

References

[1] S.S. Sazhin, Advanced models of fuel droplet heating and evaporation, Prog. Energy Combust. Sci. 32 (2006) 162-214.

[2] A.M. Lippert, Modelling of multicomponent fuels with application to sprays and simulation of Diesel engine cold start, PhD Thesis, University of Wisconsin, Madison, 1999.

[3] C. Habchi, V. Ebrahimian, Gravitational Effects on Multi-component Droplet Evaporation, Microgravity - Science and Technology 06/2012; 24(3):229-235.

[4] L.M. Pickett, D.L. Siebers, Non-Sooting, Low Flame Temperature Mixing-Controlled DI Diesel Combustion. SAE Technical Paper, No. 2004-01-1399, 2004.

[5] Zhang, L., Kong, S.-C., Multicomponent vaporization modeling of bio-oil and its mixtures with other fuels, Fuel 95 (2012) 471–480.

[6] G.M. Faeth, Evaporation and combustion of sprays, Prog. Energy Combust. Sci. 9 (1983) 1–76.

[7] A.Y. Tong, W.A. Sirignano, Multicomponent transient droplet vaporization with internal circulation: integral equation formulation, Numer. Heat Transfer 10 (1986) 253–278.

[8] P.L.C. Lage, C.M. Hackenberg, R.H. Rangel, Nonideal vaporization of dilating binary droplets with radiation absorption, Combust. Flame 101 (1995) 36–44.

[9] D.J. Torres, P.J. O'Rourke, A.A. Amsden, Efficient multi-component fuel algorithm, Combust. Theory Model. 7 (2003) 67–86.

[10] C. Maqua, G. Castanet, F. Lemoine, Bi-component droplets evaporation: temperature measurements and modelling, Fuel 87 (2008) 2932–2942.

[11] J. Tamim, W.L.H. Hallett, Continuous thermodynamics model for multicomponent vaporization, Chem. Eng. Sci. 50 (1995) 2933–2942.

[12] A.M. Lippert, R.D. Reitz, Modelling of Multicomponent Fuels using Continuous Distributions with Application to Droplet Evaporation and Sprays, SAE Technical Paper 972882, 1997.

[13] G.-S. Zhu, R.D. Reitz, A model for high-pressure vaporization of droplets of complex liquid mixture using continuous thermodynamics, Int. J. Heat Mass Transfer 45 (2002) 495–507.

[14] M. Burger, R. Schmehl, K. Prommersberger, O. Schäfer, R. Koch, S. Wittig, Droplet evaporation modelling by the distillation curve model: accounting for kerosene fuel and elevated pressures, Int. J. Heat Mass Transfer 46 (2003) 4403–4412.

[15] C.K. Law, H.K. Law, A d2-law for multicomponent droplet vaporization and combustion, AIAA J. 20 (1982) 522–527.

[16] S.K. Aggarwal, H.C. Mongia, Multicomponent and high-pressure effect on droplet vaporization, J. Eng. Gas Turbines Power 124(2) (2002), 248-255.

[17] S.S. Sazhin, J.-F. Xie, I.N. Shishkova, A.E. Elwardany, M.R. Heikal, A kinetic model of droplet heating and evaporation: Effects of inelastic collisions and a non-unity evaporation coefficient, International Journal of Heat and Mass Transfer 56 (2013) 525–537.

[18] S.S. Sazhin, A.E. Elwardany, P.A. Krutitskii, V. Deprédurand, G. Castanet, F. Lemoine, E.M. Sazhina, M.R. Heikal, Multi-component droplet heating and evaporation: Numerical simulation versus experimental data, International Journal of Thermal Sciences 50 (2011) 1164-1180.

[19] G. Brenn, L.J. Deviprasath, F. Durst, C. Fink, Evaporation of acoustically levitated multi-component liquid droplets, International Journal of Heat and Mass Transfer 50 (2007) 5073–5086.

[20] S.S. Sazhin, A. Elwardany, P.A. Krutitskii, G. Castanet, F. Lemoine, E.M. Sazhina, M.R. Heikal, A simplified model for bi-component droplet heating and evaporation, International Journal of Heat and Mass Transfer 53 (2010) 4495–4505.

[21] Abramzon, B., Sirignano, W.A.: Droplet vaporization model for spray combustion calculations, International Journal of Heat and Mass Transfer 32(9), 1605–1618 (1989).

[22] S. Bird, Transport Phenomena, Lightfoot, 2002.

[23] I.G. Gusev, P.A. Krutitskii, S.S. Sazhin, A.E. Elwardany, New solutions to the species diffusion equation inside droplets in the presence of the moving boundary, International Journal of Heat and Mass Transfer 55 (2012) 2014–2021.

[24] S. Tonini, G.E. Cossali, An analytical model of liquid drop evaporation in gaseous environment, Int. J. Therm. Sci. 57 (2012) 45–53.

[25] J.C. Slattery, Momentum, Energy and Mass Transfer in Continua, second ed., vol. 482, R. Krieger Publ., New York, 1981.

[26] M.A. Blanc, J.Phys, 7, 825, 1908.

[27] M.C. Yuen, L.W. Chen, On drag of evaporating droplets, Combust. Sci. Tech. 14 (1976) 147-154.

[28] J. Wilms, Evaporation of Multicomponent Droplets, PhD Thesis, Universität Stuttgart, 2005.

[29] B.E. Polling, J.M. Prausnitz, J.P. O'Connell, The Properties of Gases and Liquids. McGraw-Hill, 2000.

Table1

Click here to download high resolution image

Alcohol and acetone

composition	A1	A2	A3
ethanol	0.25	0.5	0.75
acetone	0.75	0.5	0.25

Table2

Click here to download high resolution image

Alkane and ketone

composition	B1	B2	B3
n-decane	0.85	0.9	0.95
3-pentanone	0.15	0.1	0. 5

Table3

Click here to download high resolution image

Alcohols, alkanes and water

composition	C1	C2	C3	C4
methanol	0.2	0.2	0.3	0.25
ethanol	0.3	0.2	0.2	0.25
1-butanol	0.3	0.2	0.2	0.25
n-heptane	0.2	0.2	0.15	-
n-decane	-	0.2	0.15	-
water	-	-	-	0.25

Table4

Click here to download high resolution image

Alkanes

composition	D1(m)	D2	D3	D4	D5(m)	D6	D7
n-octane	-	-	-	-	-	0.33	0.33
n-decane	-	-	-	-	-	0.33	-
n-dodecane	-	-	-	-	-	0.33	0.33
n-tetradecane	1.	0.8	0.6	0.4	0.	-	-
n-hexadecane	0.	0.2	0.4	0.6	1.	-	0.33

Figure1

Click here to download high resolution image

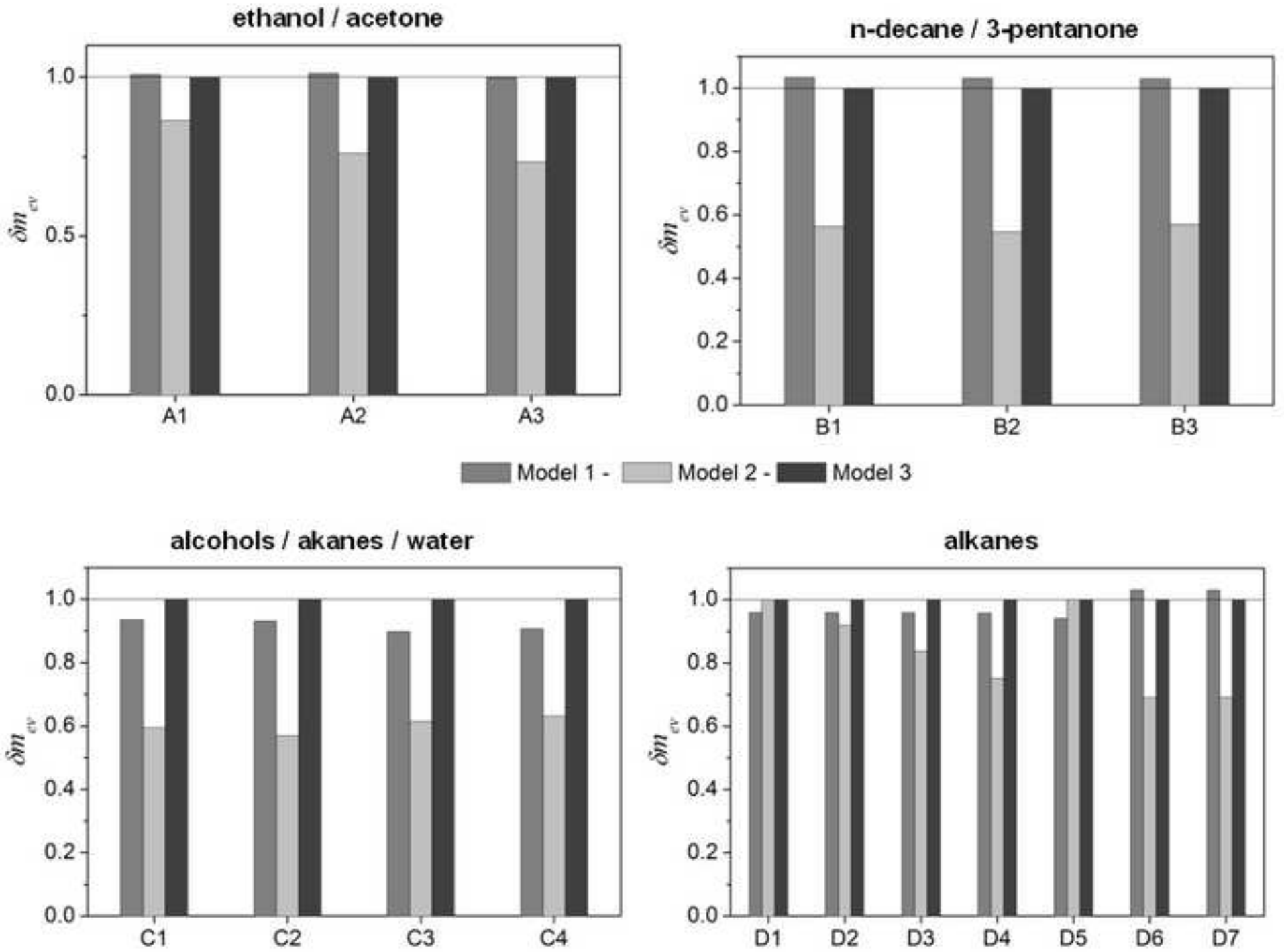

Figure2

Click here to download high resolution image

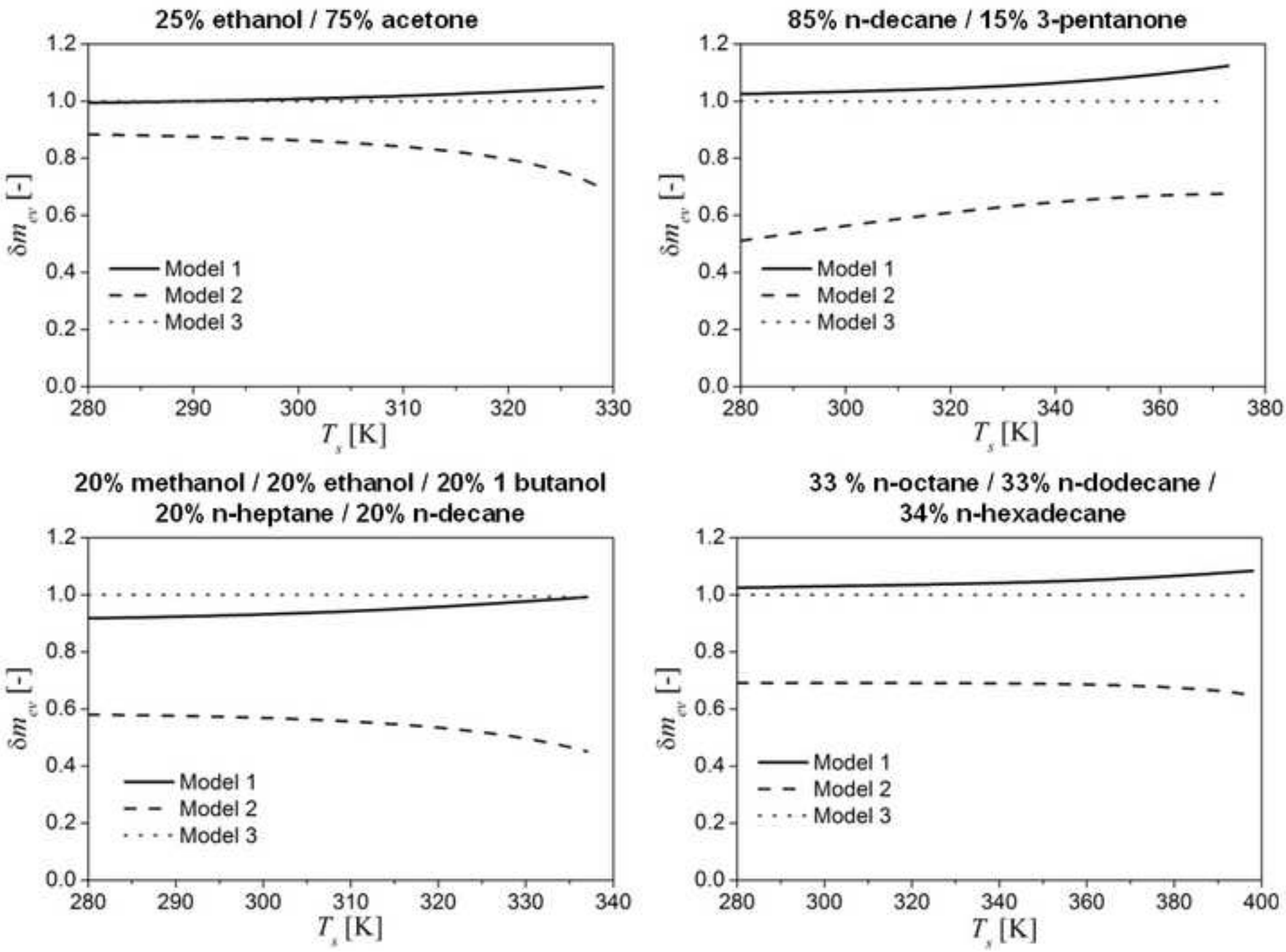

Figure3

Click here to download high resolution image

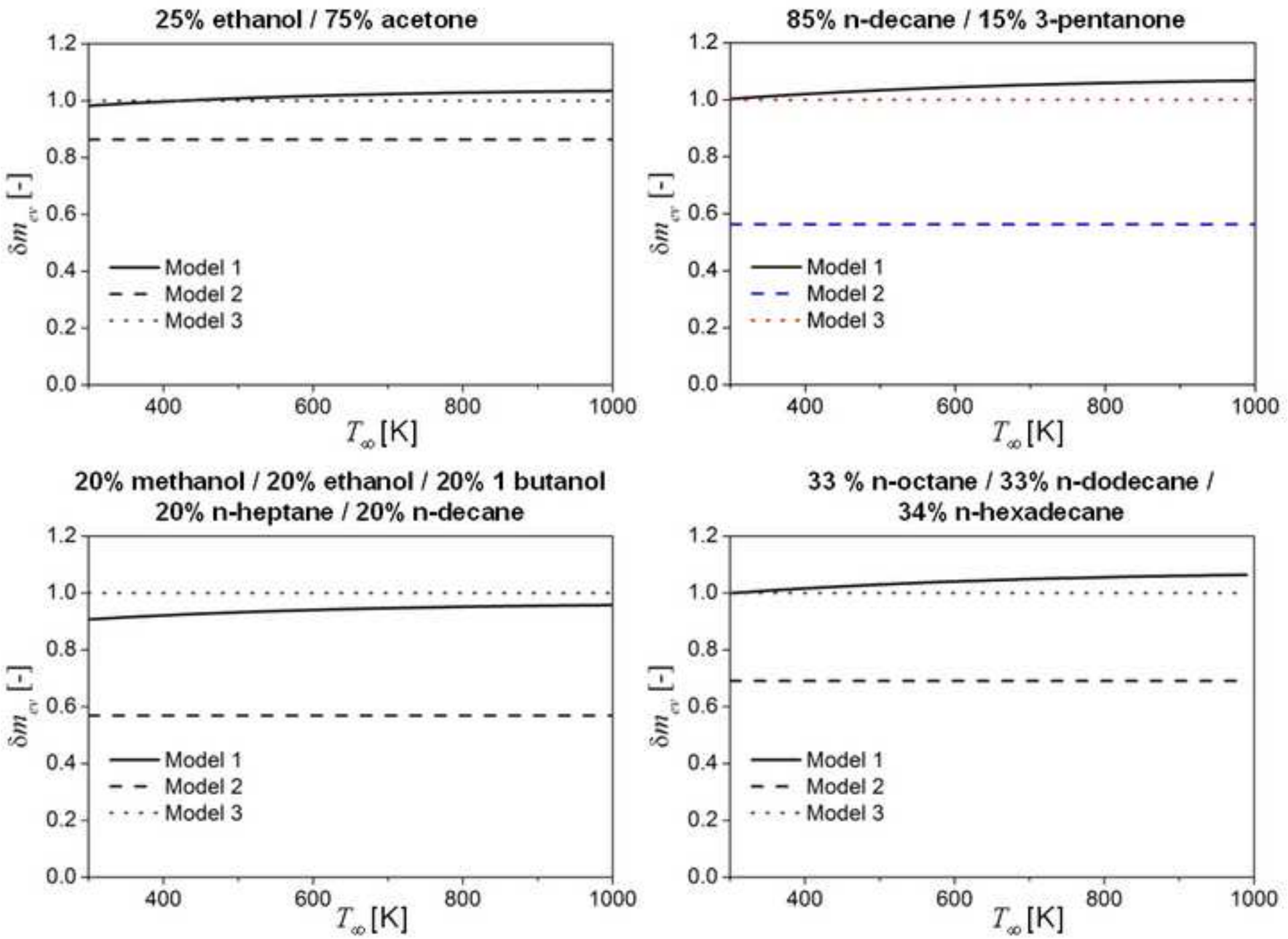

Figure4

Click here to download high resolution image

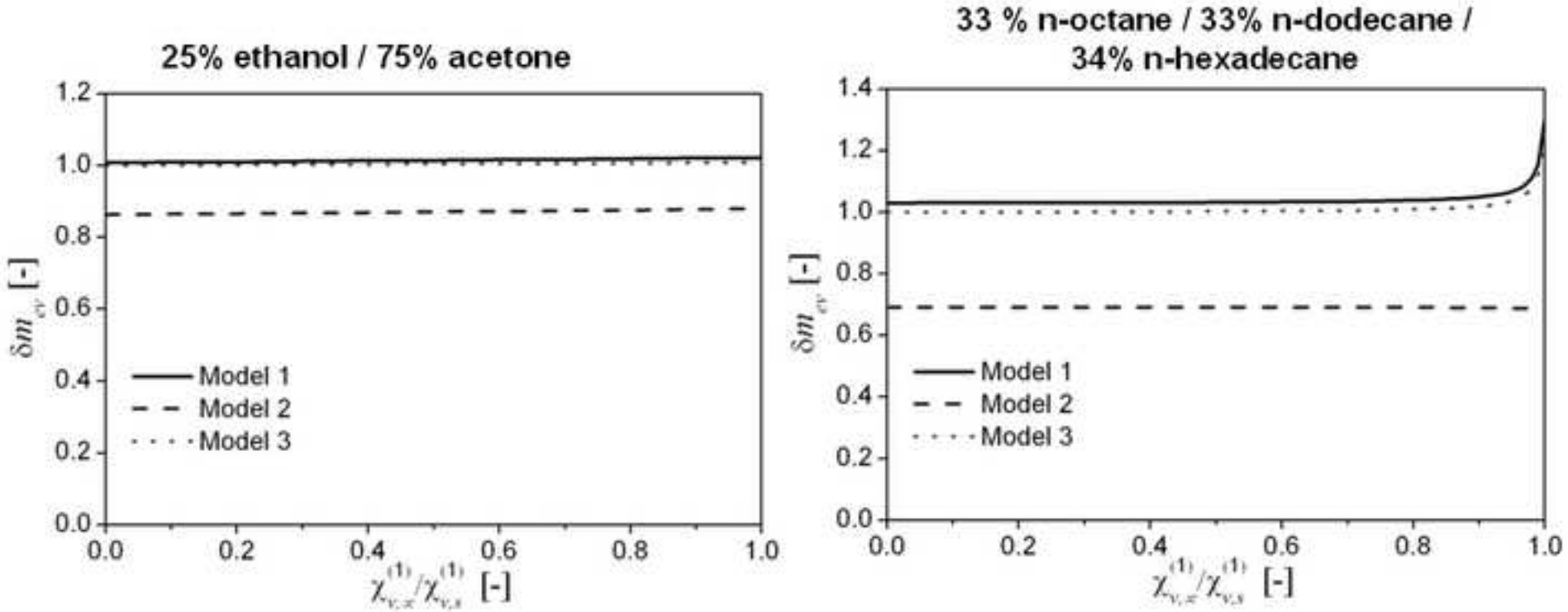

Figure5

Click here to download high resolution image

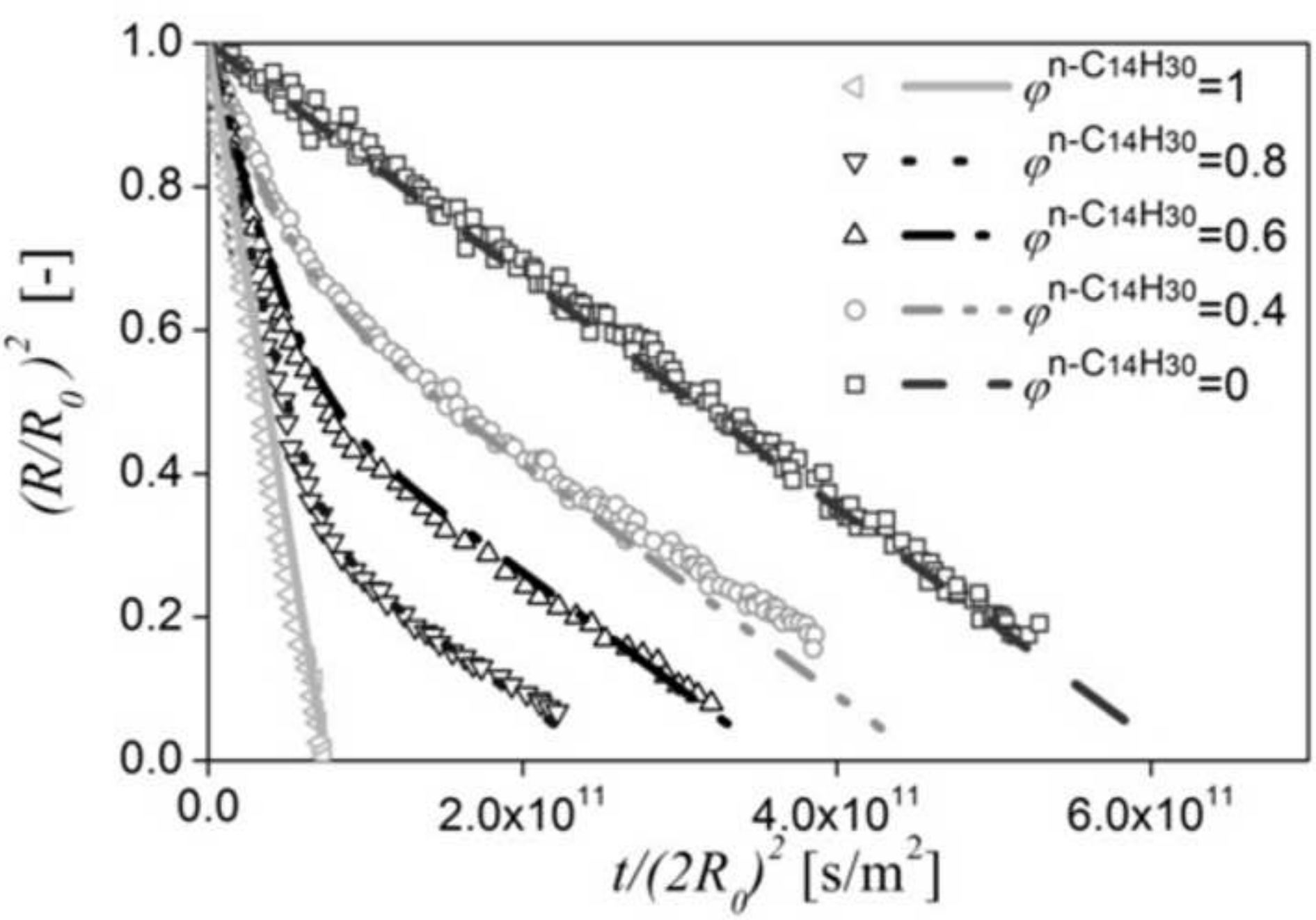

Figure6

Click here to download high resolution image

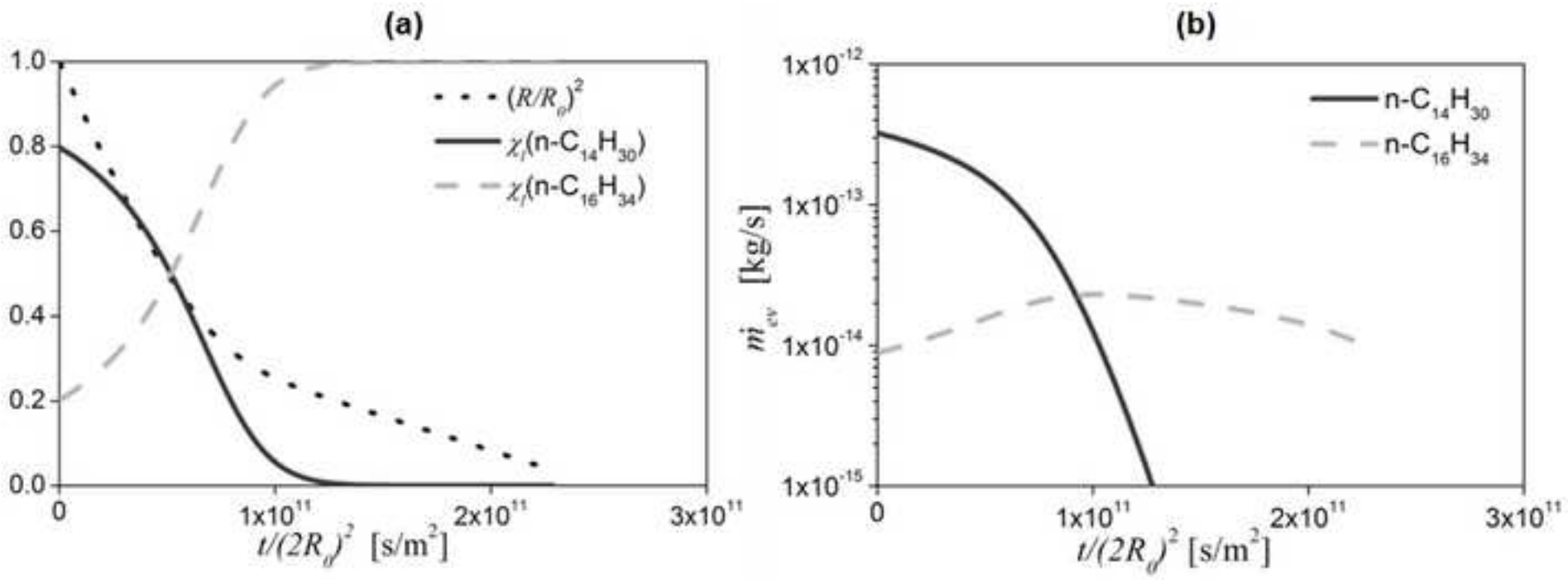

Figure7
Click here to download high resolution image